Tgif and *Smad2* mutations increase mammalian sensitivity to retinoic acid teratogenesis

A Senior Honors Thesis

Presented in partial fulfillment of the requirements for graduation
with distinction in Molecular Genetics in the undergraduate colleges
of The Ohio State University

by

Samuel Lasse

The Ohio State University
June 2005

Project Adviser: Doctor Michael Weinstein, Department of Molecular Genetics

Thesis Committee:

Dr. Michael Weinstein
Dr. Susan Cole
Dr. Christine Beattie

Abstract

Mouse model systems have proven very useful in the study of human birth defects. Such is the case for holoprosencephaly (HPE), which results from improper division of the forebrain. One gene that has been associated with human cases of HPE is TG-interacting factor (*TGIF*). This gene was first discovered through its ability to bind retinoid X receptor response elements and repress retinoid X receptor-α mediated transcription**.** Breeding mice possessing a targeted null allele of *Tgif* reveals that *Tgif* mutations alone do not result in HPE. Instead, *Tgif* mutations may be required in conjunction with other genetic mutations or environmental factors in order to cause HPE. Previous studies showing that prenatal exposure to retinoic acid (RA) results in HPE sparked interest in the function of *Tgif* in RA signaling. Teratogenesis experiments demonstrate that *Tgif* mutations result in an increased susceptibility to HPE development through overexposure to all-trans retinoic acid (ATRA). These results represent a novel cooperation between environmental and genetic factors in the etiology of HPE. Because *Tgif* has also been implicated in transforming growth factor β (TGF-β) signaling, similar teratogenesis experiments were performed with mice harboring null mutations in *Smad2*, a TGF-β signal transducer that physically interacts with *Tgif*. Heterozygous loss of Smad2 also results in a predisposition to developing HPE through ATRA teratogenesis. Analyses using a retinoid responsive *lacZ* reporter gene provide evidence that embryonic day 9.5 and 10.5 embryos with *Tgif* or *Smad2* mutations maintain an increased level of RA signaling in the forebrain. These observations support *Tgif* as a mediator of RA signaling during development and imply a novel interaction between RA and TGF-β signaling.

Table of Contents

List of Tables

List of Figures

Abbreviations

9cisRA	9-cis retinoic acid
ATRA	all-trans retinoic acid
BMP	bone morphogenic protein
co-Smad	common-mediator Smad
DMEM	Dulbecco's modified Eagle's medium
E	embryonic day
FCS	fetal calf serum
HPE	holoprosencephaly
I-Smad	inhibitory Smad
NLS	nuclear localization sequence
PBS	phosphate buffered saline
R-Smad	receptor-regulated Smad
RA	retinoic acid
RAR	retinoic acid receptor
RARE	retinoic acid receptor response element
RXR	retinoid X receptor
RXRE	retinoid X receptor response element
SHH	Sonic Hedgehog
TGF-β	transforming growth factor beta
TGIF	TG-interacting factor

Chapter 1

Introduction

The first step to preventing any human ailment is understanding the mechanism through which it develops. Genetic diseases are defined as ailments due to DNA mutations or cooperation between mutations and environmental influences. There are two main strategies for elucidating which specific mutations are responsible for a genetic disease. First, one may start with a phenotypic subject, search their DNA sequence for mutations or deletions, and correlate them with the DNA sequences of other affected subjects. The second strategy involves altering the genome of a subject and observing whether the alteration is sufficient for causing the disease. This second strategy, however, remains unethical to use on human subjects. Instead, many researchers turn to mice for these purposes because of their genetic malleability, relatively short generation time, and high degree of comparability to humans.

Mouse strains harboring mutations in genes such as *Tgif* , *Smad2*, or *Smad3* not only aid in understanding the mechanisms of genetic disease, but also reveal functions of the targeted gene in proper embryonic development.

1.1 Forebrain formation and holoprosencephaly

Nervous system development in humans is similar to that in mice and can be thought of as a specified sequence of events. After initial patterning, the neural plate invaginates and the sides fuse together forming a cylindrical structure called the neural

tube, which will later give rise to the central nervous system (Figure 1.1). This occurs around days 24-26 of human gestation and embryonic days 8.0 to 9.0 (E8.0-E9.0) of mouse gestation (Reviewed in [1]). Next, the anterior portion of the neural tube begins to form the prosencephalon, which will eventually become the forebrain. Around week 5-6 in humans and E9.0 –E10.0 in mice, the prosencephalon undergoes 3 cleavages: horizontal, transverse, and sagittal. The horizontal cleavage causes formation of paired optic vesicles, olfactory bulbs, and tracts. The transverse cleavage separates the diencephalon and the telencephalon. Finally, the sagittal cleavage divides the telencephalon into two portions, which will eventually form the right and left hemispheres of the forebrain (Reviewed in [1]) (Figure 1.2). The events that occur during the patterning of the prosencephalon influence the formation of the forebrain and certain facial features. Therefore, many birth defects that affect the forebrain and face begin at this stage. A few examples of these are aprosencephaly, atelencephaly, and holorosencephaly (HPE). Although the least severe of the three, HPE is the most common of these birth defects, occurring in 1 out of every 250 conceptions [2]. However, due to the high rate of lethality, HPE is only seen in 1 out of every 16000 live births [3]. The majority of HPE cases result from a failure of the sagittal cleavage of the telencephalon to initiate or complete (Reviewed in [1]). This leaves the hemispheres of the forebrain in a fully to partially fused state, characteristic of HPE. Other anomalies that may accompany HPE include cyclopia, mental retardation, cleft palate, and minor midline abnormalities [4] (Figure 1.3). Cases of HPE are classified into one of three groups: alobar, semilobar, or lobar, ranging from most to least severe [5].

The etiology of HPE is very diverse, containing both genetic and environmental factors. Currently there are at least 12 human genetic loci associated with HPE and 11 genes including Sonic Hedgehog *(SHH)* and *TGIF* [6]. *SHH* is expressed in the ventral midline of the developing forebrain [7] and is required for proper formation of brain, eyes, somites, spinal cord, craniofacial structures, and limbs [8]. Moreover, *SHH* mutations in humans result in HPE [9, 10], and mice with targeted null alleles of *Shh* display limb defects, midline defects, abnormal forebrain formation, and cyclopia [10]. *TGIF* was first characterized, using a human liver cDNA expression library, for its ability to bind the *cellular retinol-binding protein II* (*CRBPII*) promoter sequence. The specific motif recognized by TGIF overlaps the retinoid X receptor response element (RXRE) contained in the *CRBPII* promoter. In this context TGIF was found to reduce retinoid X receptor-α (RXRα) mediated transcriptional activation through direct competition for binding to the RXRE site [11]. *TGIF*'s involvement in the development of HPE was identified through analysis of chromosomal deletions in patients displaying HPE [12]. Alterations of transforming growth factor β (TGF-β) signaling have also been associated with HPE-like abnormalities in mice and zebrafish (reviewed in [6]). Environmental causes of HPE include ethyl alcohol, cyclopamine, and retinoic acid (reviewed in [13]).

1.2 Retinoic acid signaling

Retinoic acid (RA), a biological derivative of vitamin A, performs a vital role in many aspects of embryonic development including limb formation, specification of the anterior-posterior axis, skeletal development [14], and cellular differentiation (reviewed in [15]). The great diversity of functions carried out by RA signaling is better understood

through its signaling mechanisms. Due to its small molecular weight and non-polarity, RA is able to permeate cell membranes unaided. It may also be synthesized from vitamin A (reviewed in [16]). Once inside the cell, the various forms of RA preferentially bind one of two nuclear receptors, the retinoic acid receptor (RAR) or the retinoid X receptor (RXR) (Figure 1.4). All-trans RA (ATRA) and 9-cis RA (9cisRA) are able to bind and activate RARs, whereas only 9cisRA is able to activate RXRs (reviewed in [15]). Once activated, RXR preferentially heterodimerizes with an activated RAR, but may also homodimerize with an RXR, in order to regulate transcription of target genes. The sequence specific binding motifs recognized by the hetero/homodimers usually contain an exact repeat of PuG(G/T)TCA or a close variation, which are separated by 1, 2, or 5 basepairs (reviewed in [15]). Adding further to the functional diversity of retinoid signaling, the RAR and RXR families each consist of three isoforms (α,β,γ) and each isoform contains at least two different splice variants, totaling 8 RAR proteins and 6 RXR proteins. The resulting 48 possible heterodimers and numerous homodimers help to explain the wide role that retinoid signaling plays in embryonic development (reviewed in [15]).

1.3 TGF-β signaling

TGF-β signaling plays an important role in development as well. Depending on the context, TGF-β signaling can cause cellular proliferation, apoptosis, or differentiation, and maintains a vital function in gastrulation and dorsoventral patterning [17]. Perturbations in TGF-β signaling have even been associated with murine cases of HPE-like cyclopia (reviewed in [6]). The TGF-β superfamily contains many activators

such as TGF-β ligands, nodal, activins, and bone morphogenic proteins (BMPs), each signaling through a set of serine/threonine receptors named TGF-β receptor type I and type II (Figure 1.5) (reviewed in [18]). Upon binding the type II receptor, the resulting ligand-receptor complex recruits a type I receptor and subsequently phosphorylates it (reviewed in [18]). The activated type I receptor can then activate a number of Smad proteins to relay the signal to the nucleus. The Smads are a diverse group of proteins including 8 known members, Smad1 through Smad8. There are three types of Smads: inhibitory Smads (I-Smads), common-mediator Smad (co-Smad), and receptor-regulated Smads (R-Smads). I-Smads include Smad6 and Smad7, and the co-Smad is Smad4. R-Smads are divided into two subgroups by ligand specificity; Smad2 and Smad3 are activated by TGF-β ligands, activins, or nodal, whereas Smad1, Smad5, and Smad8 are activated by BMPs (reviewed in [18]). The R-Smads and co-Smad each contain conserved MH1 and MH2 domains (Figure1.6). The MH1 domain carries DNA binding capabilities in all but Smad2, in addition to a nuclear localization sequence (NLS) with the exception of Smad4 (reviewed in [18]). The MH2 domain contains the serine-rich activation site and provides the ability to complex with other Smad proteins as well as the TGF-β receptors. Once the type I receptor is activated, it phosphorylates an R-Smad, which then complexes with Smad4. Upon phosphorylation, conformational changes in the R-Smad protein structure open the NLS and allow translocation into the nucleus (reviewed in [18]). It is this point in the pathway where the I-Smads are able to produce their inhibitory effects. Because they retain the MH2 domain and its protein interaction capabilities, they can compete with R-Smads for binding of the TGF-β receptors (reviewed in [18]).

Once the R-Smad/Smad4 complex has entered the nucleus it recognizes specific DNA sequences and recruits transcriptional mediators such as CBP/p300. These acetyltransferases loosen the DNA chromatin structure and promote gene transcription (reviewed in [18]). However, other mediators such as Tgif, Ski, and c-Jun [19-21] can recruit histone deacetylases, which tighten the DNA structure and prevent gene transcription. My study focuses on Tgif specifically. Although discovered for its activity in retinoic acid signaling, Tgif can also be recruited by and bind to Smad2. It is a homeodomain protein, which refers to a relatively conserved sequence of amino acids called the homeodomain and typically confers involvement in transcriptional activation or repression [22].

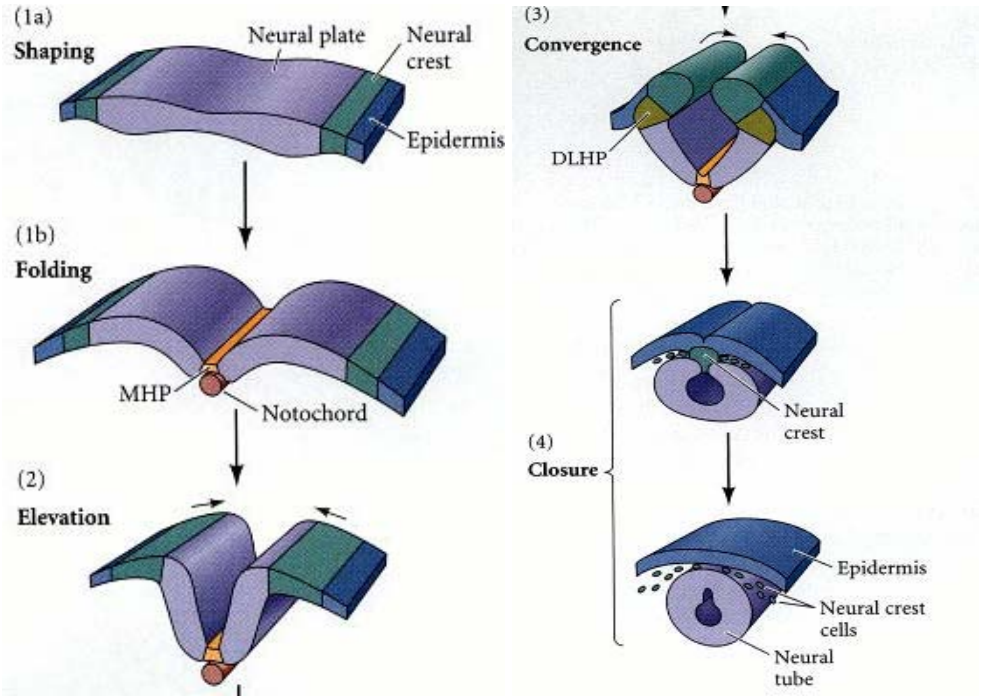

Figure1.1 Mammalian neurulation. As shown above, the Neural plate invaginates and the sides converge to form the Neural tube. This occurs around days 24-26 of human gestation and E8.0-E9.0 of mouse gestation. Taken from [14].

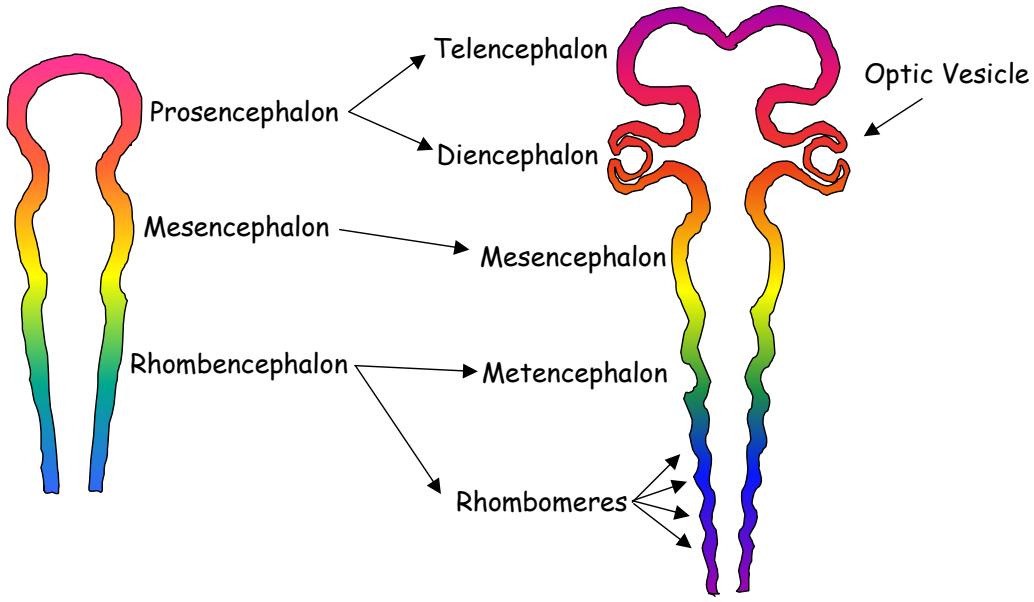

Figure1.2 Mammalian prosencephalon development. During weeks 5 and 6 of human gestation, the prosencephalon undergoes three cleavages. The horizontal cleavage forms the optic vesicles, olfactory bulbs, and tracts. The transverse cleavage separates the diencephalon and the telencephalon. The sagittal cleavage divides the telencephalon into right and left hemispheres. Altered from [23].

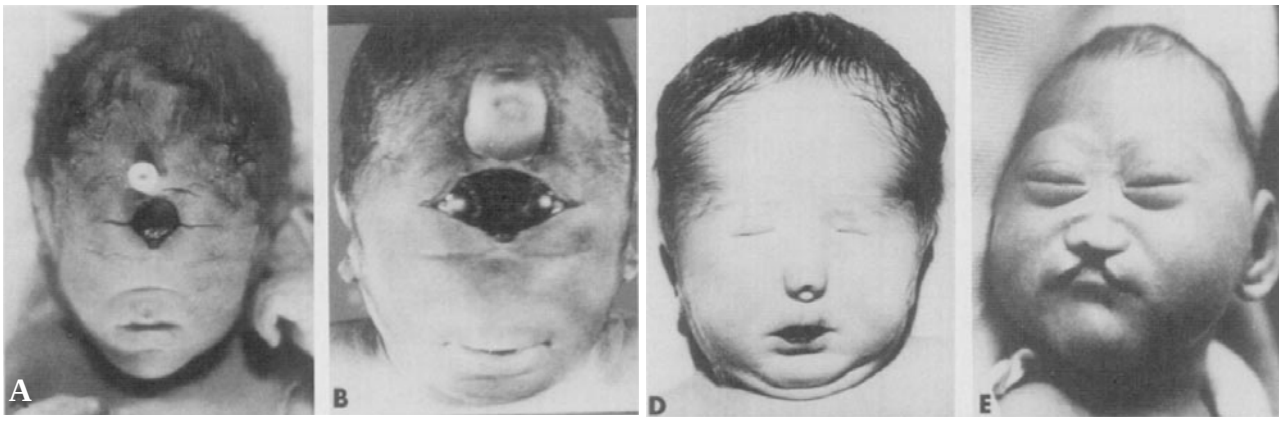

Figure1.3 Abnormalities associated with HPE. (A,B) More severe cases exhibit cyclopia and a proboscis, which is present above the eye. Less severe cases exhibit minor midline abnormalities such as a single nostril (D) and cleft lip (E). Taken from [5].

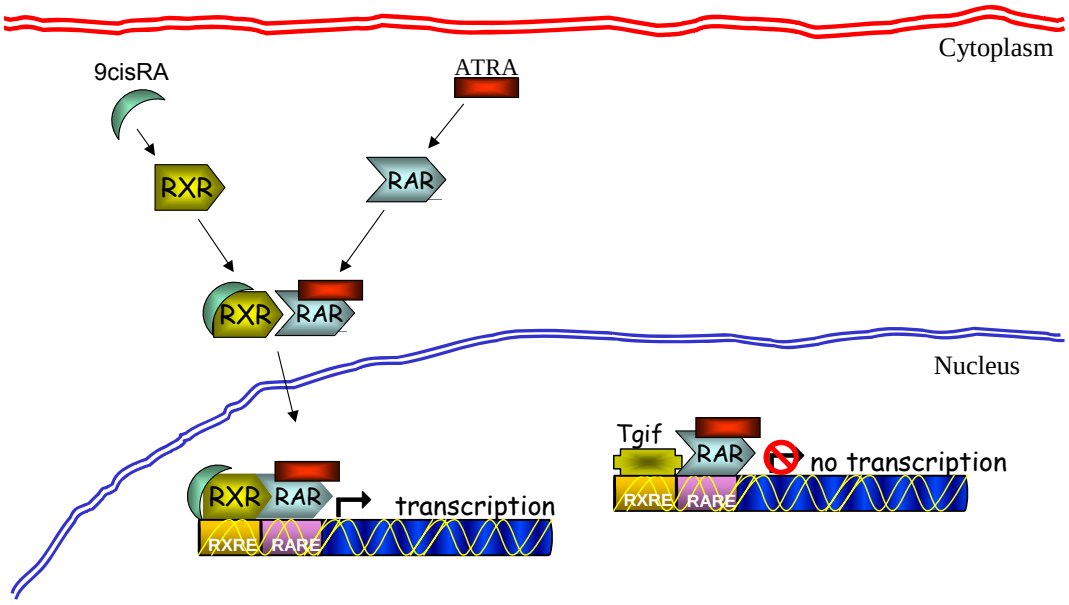

Figure1.4 Retinoic acid signaling pathway. Two forms of retinoic acid, 9-cis (9cisRA) and all-trans (ATRA), enter the cell and activate retinoid receptors through direct binding. 9cisRA may activate either the retinoic acid receptor (RAR) or the retinoid X receptor (RXR), where ATRA activates only the RAR. Activated receptors then homodimerize or more commonly heterodimerize as depicted here. Finally, the receptor complexes activate target gene transcription by recognizing the appropriate retinoid response elements. Tgif is able to compete for binding of the retinoid X receptor response element (RXRE) in order to prevent RA dependent transcription.

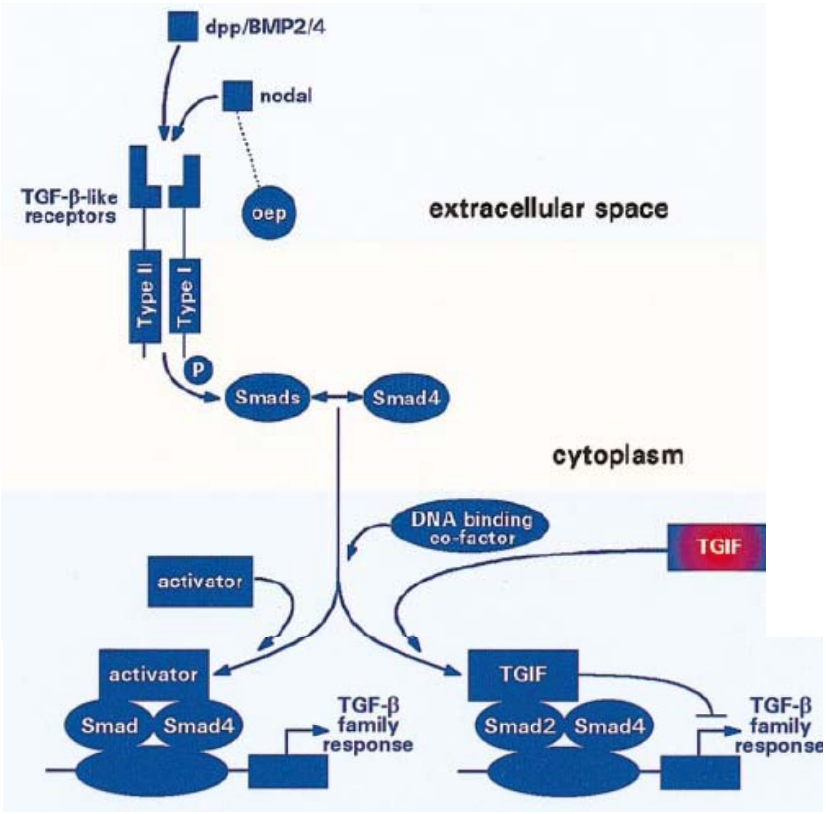

Figure1.5 TGF-β signaling pathway. Extracellular ligands bind the TGF-β type II receptor, which becomes activated and recruits a TGF-β type I receptor. The receptor complex then activates R-Smads such as Smad2. The co-Smad, Smad4, then chaperones the R-Smad into the nucleus where the Smad complex associates with co-activators or co-repressors like TGIF to regulate target gene transcription. Taken from [6].

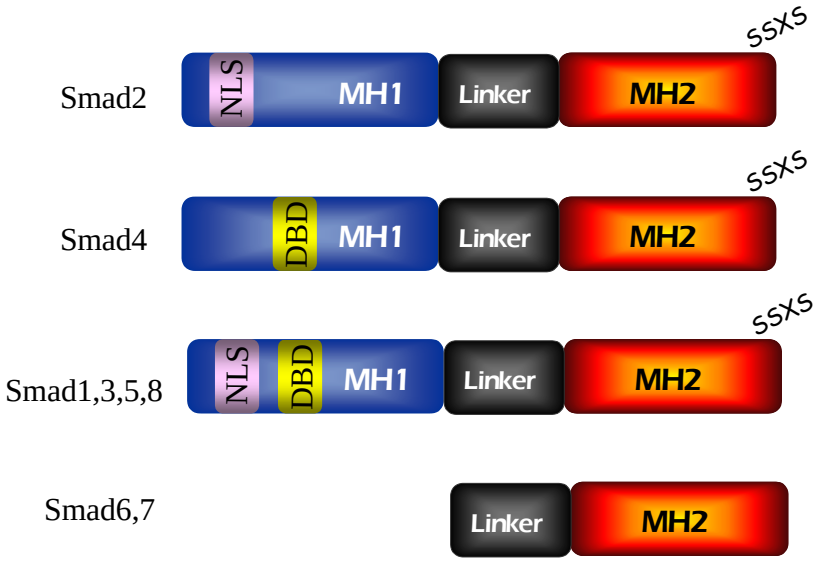

Figure1.6 Smad protein structure. Except for Smads 6 and 7, the Smad proteins all contain conserved MH1 and MH2 domains connected by a linker region. The MH1 domain carries a nuclear localization sequence (NLS) in all but Smad4. It also encodes a DNA binding domain (DBD) in all but Smad2. The MH2 domain contains a serine-rich activation site, and facilitates protein-protein interactions.

Chapter 2

Introduction

Many genes have multiple functions, such as the *Drosophila* gene *Dichaete*. This gene has been found to function in fly segmentation, development of the central nervous system, brain, and hindgut, as well as post-embryonic development [24-26]. Because homozygous null mutations of the *Dichaete* gene are lethal, its full range of functions must be deduced through means other than null mutations. These methods typically include the use of hypomorphic alleles, artificially regulated alleles, or combining genetic mutations of related genes. A similar situation exists with the murine gene *Smad2*. *Smad2* homozygous null mice (*Smad2* $^{-/-}$) are lethal before E8.5, while 95% of mice heterozygous for the *Smad2* null mutation (*Smad2* $^{+/-}$) show no phenotype [27, 28]. The remaining 5% display gastrulation defects at E9.5 [28]. The *Smad2* $^{-/-}$ embryos also fail to gastrulate and therefore suggest a role for Smad2 during gastrulation [27], but unfortunately it also means that the functions of *Smad2* cannot be deduced past E9.5 through use of a *Smad2* null mutation alone. For this reason, Ye Liu of the Weinstein laboratory bred *Smad2* and *Smad3* mutant strains together. Although *Smad2* $^{+/-}$ mice and *Smad3* $^{+/-}$ mice are both viable, 51% of *Smad2* $^{+/-}$; *Smad3* $^{+/-}$ mice exhibit embryonic lethality. Furthermore, over 82% of *Smad2* $^{+/-}$; *Smad3* $^{+/-}$ embryos survive past E8.5, and 44% of E9.5 - E10.5 embryos exhibit craniofacial or midline defects such as HPE [28]. These results allow Liu *et al.* to conclude that *Smad2* and

Smad3 function in endodermal specification and migration, leading to proper craniofacial and midline patterning [28].

2.1 *Tgif* ; *Smad2* mutant embryos display holoprosencephaly

To further elucidate the role of *Smad2* during murine development, Dr. Tessa Carrel of the Weinstein laboratory combined *Smad2* mutations with null mutations in the murine gene *Tgif*. Tgif was chosen because of its interaction with Smad2 and Smad3 in TGF-β signaling, and more importantly, its connection with human cases of HPE [29]. The *Tgif* mutant strain was obtained from Dr. David Wotton at the University of Virginia. Breeding of *Tgif* heterozygotes produces live born pups in mendelian ratios, and *Tgif* $^{-/-}$ mice are viable and fertile (data not shown). To confirm the successful targeted disruption of the gene, whole mount *in situ* hybridization analysis was performed on E9.5 *Tgif* $^{-/-}$ embryos and found to have no *Tgif* expression relative to wild type embryos (Maria Festing unpublished data). Whole mount analysis of wild type embryos at E8.5 and E9.5 reveals *Tgif* expression along the anterior edge of the developing telencephalon at E8.5 and through out the prospective forebrain at E9.5 (Maria Festing submitted) (Figure 2.1). These expression patterns make *Tgif* an excellent candidate for involvement in the occurrence of holoprosencephaly.

The combination of *Smad2* and *Tgif* null alleles again produced embryonic lethality in the double heterozygous mice as well as *Smad2*$^{+/-}$; *Tgif* $^{-/-}$ mice. Also as before, craniofacial defects such as HPE were observed in E9.5 - E10.5 embryos (Dr. Tessa Carrel unpublished data). However, upon further investigation, the basis for holoprosencephalic defects appeared to differ between *Smad2*; *Smad3* and *Smad2*;

Tgif embryos. Using whole mount *in situ* analysis, it was determined that *Smad2* $^{+/-}$; *Smad3* $^{+/-}$ embryos displaying midline abnormalities show a reduced rostral expression of *Shh*, *Otx2*, and *Fgf8*, each involved in the development of the forebrain or midbrain structures [28]. Conversely, abnormal *Smad2* $^{+/-}$; *Tgif* $^{+/-}$ and *Smad2* $^{+/-}$; *Tgif* $^{-/-}$ embryos only show a loss of rostral expression of *Otx2* and display no change in *Shh*, *Fgf8*, or *Zic2* expression (Dr. Tessa Carrel unpublished data). These differences led to the conclusion that each combination of mutations causes HPE through different mechanisms.

2.2 *Tgif* ; *Smad3* mutant embryos fail to exhibit abnormalities

Another approach to determine the role of *Tgif* and *Smad* mutations in the causation of HPE was to cross the *Tgif* null and *Smad3* null strains. Because *Smad3* $^{+/-}$; *Tgif* $^{+/-}$ and *Smad3* $^{+/-}$; *Tgif* $^{-/-}$ mice are both viable and fertile, I was able to design crosses to obtain embryos of all allelic combinations of these two genes. Initially, 130 embryos were observed at E10.5, and a specific midbrain and hindbrain defect (Figure 2.2) was observed at an average rate of 10% over all genotypes observed (Table 2.1). A smaller percentage of other various midline abnormalities were also seen (Table 2.1). The nature of the midbrain and hindbrain phenotype warranted ruling out the possibility of it being a dissection artifact. To further investigate this phenotype, 53 embryos from similar crosses were observed at E11.5, a stage where embryos are larger and easier to dissect. At E11.5, no abnormalities were found when 8 to 9 were expected according to the percentage seen in E10.5 embryos (Table 2.2). Using a χ^2 test, the P value

obtained for the E11.5 embryos is $p<0.005$, suggesting that these results are significant and the combination of *Tgif* and *Smad3* mutations does not confer an overt phenotype.

2.3 Materials and Methods

2.3.1 Mice and Matings

Mice carrying either *Smad3* [30] or *Tgif* mutations were intercrossed and the resulting progeny were used to obtain embryos of the following genotypes: *Smad3* $^{+/+}$; *Tgif* $^{+/-}$, *Smad3* $^{+/+}$; *Tgif* $^{-/-}$, *Smad3* $^{+/-}$; *Tgif* $^{+/-}$, *Smad3* $^{+/-}$; *Tgif* $^{-/-}$, *Smad3* $^{-/-}$; *Tgif* $^{+/-}$, or *Smad3* $^{-/-}$; *Tgif* $^{-/-}$. To study embryonic development, female mice were paired with males and examined daily for vaginal plugs. The morning on which plugs were seen was assumed to correspond to E0.5. At the appropriate stage of development, the embryos were dissected from their maternal decidua in 1X phosphate buffered saline (PBS). Extraembryonic membranes were removed, retaining the yolk sack for genotyping. Evaluation of embryonic phenotypes was preformed using a Zeiss Stemi SVII Apo dissecting microscope. Embryos were then photographed with an MTI 3CCD digital camera and Scion Series 7 software.

2.3.2 Genotyping

Genotypes were determined through PCR analysis. Standard reaction conditions were utilized in a total volume of 20 μl. The reaction parameters are as follows: 5 min denaturation at 95 ^{o}C; thirty five cycles of 95 ^{o}C for 30 seconds, 60 ^{o}C for 30 seconds and 72 ^{o}C for 30 seconds, and a final elongation of 10 minutes at 72 ^{o}C.

The wild-type *Smad3* allele was detected using primer 1 (5'-CCACTTCATTGCCATATGCCCTG-3') and primer 2 (5'-CCCGAACAGTTGGATTCACACA-3'). Primer 1 is located 5' to the deletion and primer 2 is located within the deletion. This primer pair amplifies a fragment of ~400 bp. The mutant allele was visualized using primer 1 and primer 3 (5'-CCAGACTGCCTTGGGAAAAGC-3'), which is located within the targeted insertion, resulting in a 250bp fragment. The wild-type *Tgif* allele was detected using primer 4 (5'-AGTCCAACTGGCCGGAATTGTCAC-3') and primer 5 (5'-CCTCAGAGTCACTGCCTGATG-3). Primer 4 is located within the first intron, 5' to the deletion. Primer 5 is located within the deletion, and together they produce a fragment of 558bp in length. The mutant allele was amplified using primer 4 and primer 6 (5'-TGGTGCAGATGAACTTCAGGGTGAG-3'), which is located within the targeted insertion, resulting in a 690 bp fragment. The Smad2 mutant allele was detected using primer 7 (5'-GAGCTGCGCAGACCTGTTAC-3') and primer 8 (5'-GAAGGGGATCCCATCTGAGT-3'), which give a ~950bp fragment. Primer 7 is 5' to the deletion, and primer 8 is 3' to the deletion.

Embryo Genotype	Total Embryos	Abnormal Embryos	Reduced Midbrain and Hindbrain	Midline Abnormalities
Smad3 $^{+/+}$ *; Tgif* $^{+/-}$	35	3 (9%)	3 (9%)	0
Smad3 $^{+/+}$ *; Tgif* $^{-/-}$	21	3 (14%)	1 (5%)	2 (10%)
Smad3 $^{+/-}$ *; Tgif* $^{+/-}$	23	2 (9%)	2 (9%)	0
Smad3 $^{+/-}$ *; Tgif* $^{-/-}$	29	7 (24%)	2 (7%)	5 (17%)
Smad3 $^{-/-}$ *; Tgif* $^{+/-}$	11	2 (18%)	2 (18%)	0
Smad3 $^{-/-}$ *; Tgif* $^{-/-}$	11	4 (36%)	3 (27%)	1 (9%)
Totals	130	21 (16%)	13 (10%)	8 (6%)

Table 2.1 Evaluation of E10.5 *Smad3* ; *Tgif* embryos. Embryos were obtained from various crosses of *Smad3* ; *Tgif* mice.

Embryo Genotype	Total Embryos	Abnormal Embryos	Expected Abnormal (based on E10.5 percentages)	Expected Reduced Midbrain and Hindbrain (based on E10.5 percentages)
Smad3 $^{+/+}$ *; Tgif* $^{+/-}$	6	0	0.5	0.5
Smad3 $^{+/+}$ *; Tgif* $^{-/-}$	24	0	3.4	1.2
Smad3 $^{+/-}$ *; Tgif* $^{+/-}$	5	0	0.5	0.5
Smad3 $^{+/-}$ *; Tgif* $^{-/-}$	10	0	2.4	0.7
Smad3 $^{-/-}$ *; Tgif* $^{+/-}$	3	0	0.5	0.5
Smad3 $^{-/-}$ *; Tgif* $^{-/-}$	5	0	1.8	1.4
Totals	53	0	8.5	5.3

Table 2.2 Evaluation of E11.5 *Smad3; Tgif* embryos. Embryos were obtained from various crosses of *Smad3* ; *Tgif* mice.

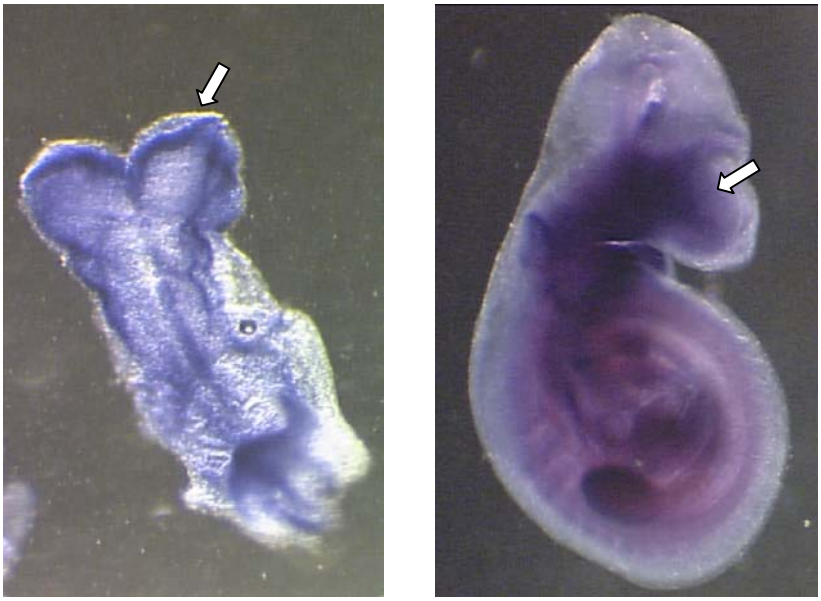

Figure 2.1 *Tgif* expression pattern at E8.5 and E9.5. The embryo on the left is E8.5 and exhibits *Tgif* expression along the anterior edge of the developing telencephalon (white arrow). The embryo on the right is E9.5 and exhibits *Tgif* expression in the prospective forebrain and craneofactial features (white arrow). Whole mounts were performed by Maria Festing.

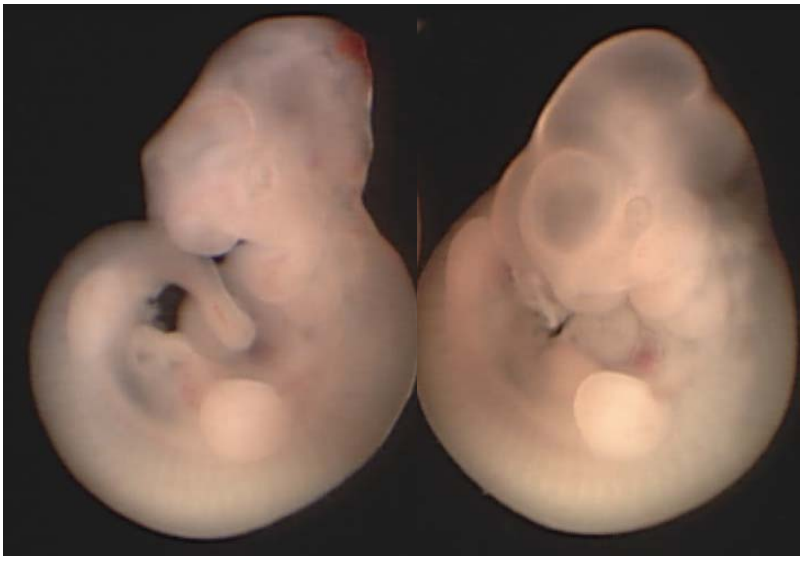

Figure 2.2 Midbrain and hindbrain phenotype of E10.5 *Smad3; Tgif* mutants. The embryo on the left is *Smad3* $^{+/-}$; *Tgif* $^{+/-}$ and exhibits the reduced midbrain and hindbrain phenotype that has been attributed to a dissection artifact. The embryo on the right is an aphenotypical littermate.

Chapter 3

Introduction

The diversity of functions that RA plays during development has led to a thorough examination of its properties. One beneficial use that has come from studying RA is its effectiveness in treating acne and wrinkles (reviewed in [31]). This in turn has led to a characterization of the much more negative teratogenic properties of RA (reviewed in [31]). A fetus exposed to high amounts of RA can develop a number of defects including HPE, which has been shown in both humans and mice [32, 33]. It is also interesting that *RXR*$\alpha^{-/-}$ mice are resistant to E11.5 exogenous exposure to RA [34]. Because of the previously mentioned evidence that Tgif is able to inhibit RXRα mediated signaling *in vitro* [11], it is hypothesized that Tgif may be required as a molecular brake on RA signaling during embryogenesis. Thus mutations in *Tgif* may function in the development of HPE through an effective increase in endogenous RA signaling or loss of an embryo's ability to respond to harmful levels of exogenous RA. In order to test this proposal, teratogenesis experiments were performed on mice with *Tgif* mutant and wild type backgrounds.

3.1 Retinoic acid teratogenesis of *Tgif* mutants

Pregnant females were intraperitoneally injected with a 7.5 mg/kg dosage of ATRA at E7.5 and embryos were observed at E10.5. This protocol is an alteration from that used by Sulik *et al*. in their study displaying the ability of RA to cause HPE in mice

[33]. Crosses were set up to produce litters of the same genotype (Figure 3.1) in order to simplify genotyping due to the relatively small size of some of the abnormal embryos. Seven litters were observed for each genotype (*Tgif* ^{wt}, *Tgif* $^{+/-}$, and *Tgif* $^{-/-}$), totaling 183 embryos. A number of abnormalities were seen, including exencephaly, hindbrain, midbrain, and forebrain reductions, as well as axial defects and HPE (Figure 3.2). The total percentage of abnormal embryos observed rose from 28% to 48% to 98% with the addition of *Tgif* mutant alleles (Table 3.1). These results strongly suggest ($p<0.01$) that *Tgif* mutations in mice provide for an increased susceptibility to ATRA teratogenesis. In order to reveal any changes in the occurrence of HPE due to differences in genotype, I separated the percentage of abnormal embryos into phenotypic subgroups (Figure 3.3). The percentage occurrence of HPE gradually increased from *Tgif* ^{wt} (2%) to *Tgif* $^{+/-}$ (7%) to *Tgif* $^{-/-}$ (12%) embryos. Although these numbers are small, the increase in percentages from *Tgif* ^{wt} to *Tgif* $^{+/-}$ ($p<0.001$) and *Tgif* ^{wt} to *Tgif* $^{-/-}$ ($p<0.001$) are statistically significant. The lack of statistical significance in the difference between *Tgif* $^{+/-}$ and *Tgif* $^{-/-}$ percentages ($0.20<p<0.30$) may be due to the small sample size, or it is possible that two *Tgif* mutations have no greater effect than one in the causation of HPE. Nonetheless, these findings illustrate that *Tgif* mutations incur a predisposition specifically to the development of HPE through ATRA teratogenesis. The importance behind this data is the characterization of a previously unknown genetic and environmental cooperation in the development of HPE.

3.2 Retinoic acid teratogenesis of *Smad2* mutants

Since *Tgif* mutations result in greater susceptibility to ATRA teratogenesis, and the combination of *Tgif* and *Smad2* mutations provide for similar abnormalities, it is possible that *Smad2* mutations also produce increased sensitivity to ATRA teratogenesis. Accordingly, experiments were performed using the same procedure as described for *Tgif* mutant embryos. The exogenous ATRA caused abnormalities in 29% of wild type embryos and 76% of *Smad2* $^{+/-}$ embryos (Dr. Tessa Carrel unpublished data). The range of abnormalities was similar to those observed in the *Tgif* teratogenesis experiment, including exencephaly, delayed growth, pericardial ballooning, and HPE (Figure 3.4). However, in this case HPE was seen at a much higher percentage in mutant embryos. Such findings bolster the proposal that mutations in *Smad2* and *Tgif* may act cooperatively to cause HPE through alterations in retinoid signaling. These results also indicate a possible role for Smad2 in the regulation of RA signaling during development.

3.3 Materials and Methods

3.3.1 Teratogenic application of retinoic acid

On E7.5, pregnant mice were injected intraperitoneally with 7.5 mg of 1 mg/ml retinoic acid in DMSO per kg of maternal body weight. This concentration was obtained from previous analyses of RA teratogenesis in mice [33]. Embryos were then isolated at E9.5 or E10.5, photographed, and examined for phenotypes.

	Tgif ^{wt}	*Tgif* $^{+/-}$	*Tgif* $^{-/-}$
Litters	7	7	7
Total Embryos	64	69	50
Normal Embryos	46	36	1
Abnormal Embryos	18	33	49
Percent Abnormal	28%	48%	98%

Table 3.1 Summary of E10.5 *Tgif* embryos exposed to ATRA. The total percentage of abnormalities seen in E10.5 embryos after ATRA treatment increased from 28% to 48% to 98% in *Tgif* ^{wt}, *Tgif* $^{+/-}$, and *Tgif* $^{-/-}$ embryos respectively.

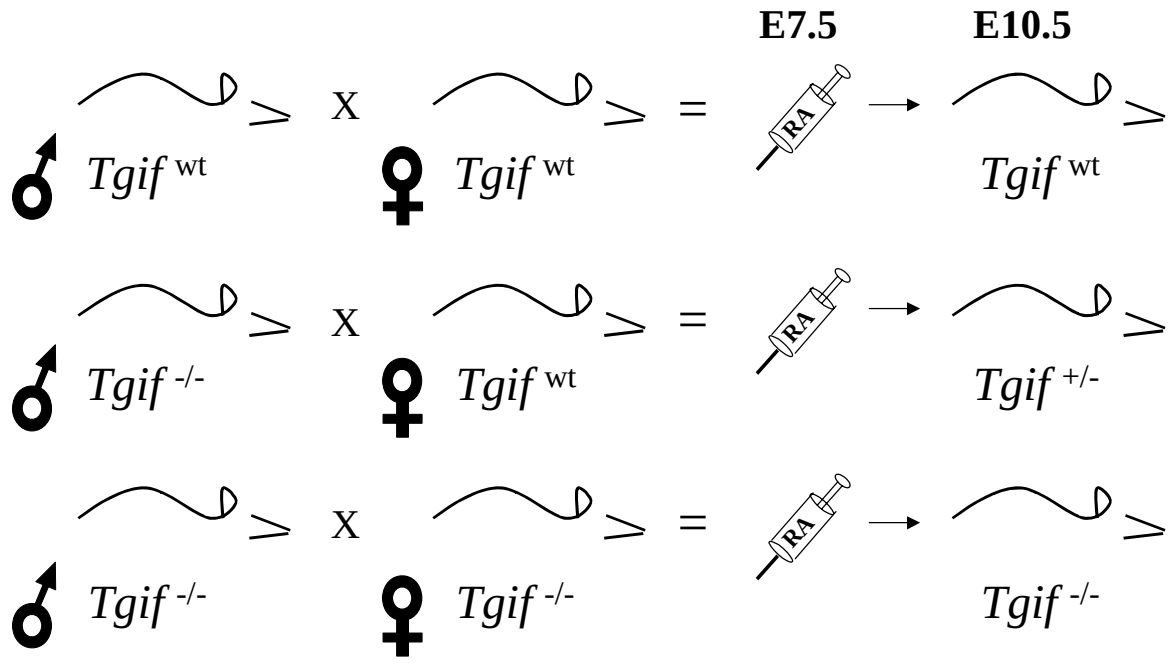

Figure 3.1 *Tgif* crosses for teratogenesis experiments. Crosses were set up to ensure that each embryo of a single litter was the same genotype. Pregnant mothers were intraperitonealy injected with 7.5mg of ATRA per 1kg of mother's weight at E7.5. Embryos were then observed for defects on E10.5.

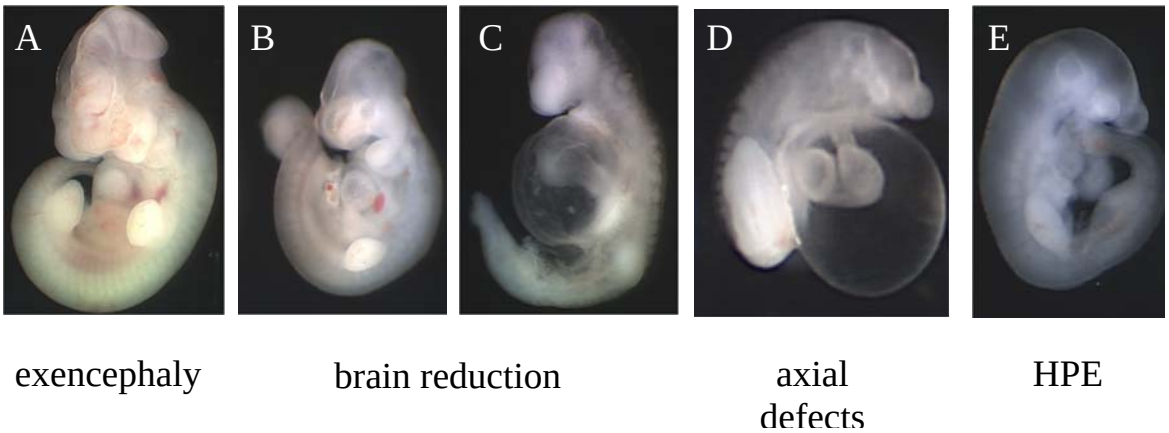

Figure 3.2 Phenotypes exhibited by E10.5 embryos exposed to ATRA. Wide ranges of phenotypes and severity were observed at E10.5. Some of the more common phenotypes include exencephaly (A), brain reductions (B, C), axial defects (D), and HPE (E).

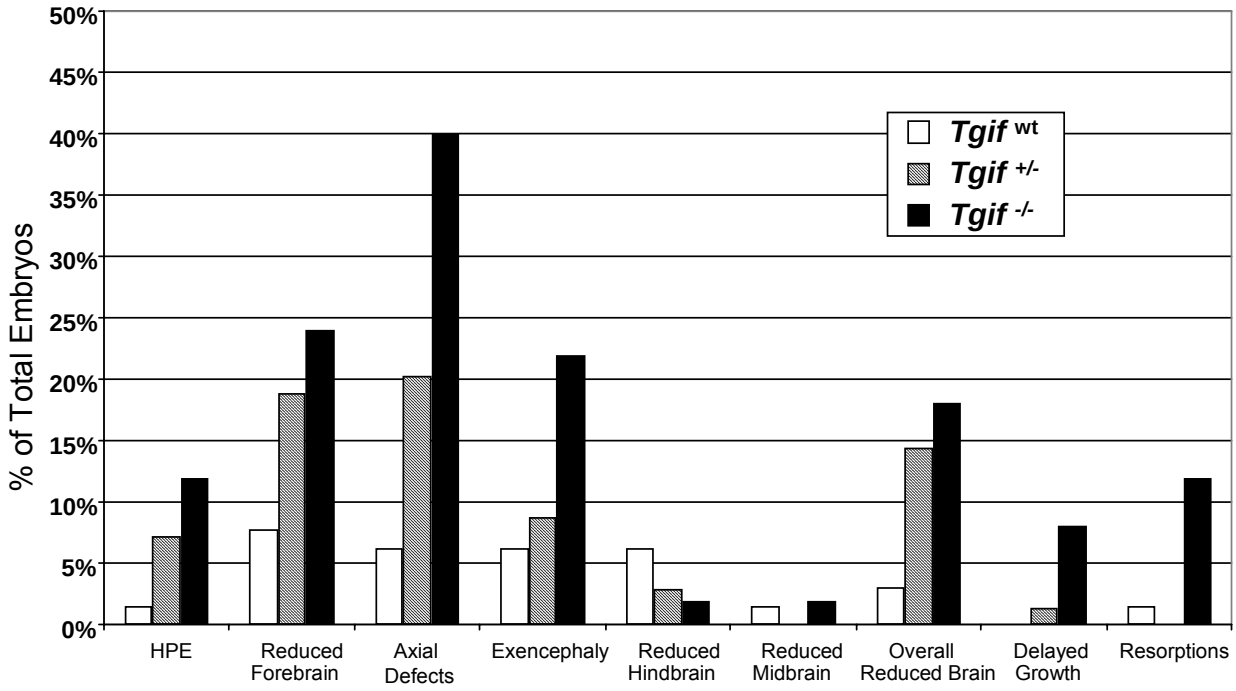

Figure 3.3 Frequency of ATRA induced abnormalities. Percentage of total embryos per genotype is plotted on the Y-axis. Note: in this chart, percentages will not add to 100% because some embryos exhibited multiple abnormalities and therefore were counted multiple times.

		normal	HPE	exencephaly	delayed growth	pericardial ballooning
Smad2 ^{wt}	embryos	12	0	5	0	0
	percentage	71%	0%	29%	0%	0%
Smad2 $^{+/-}$	embryos	4	12	3	1	1
	percentage	24%	70%	18%	6%	6%
Total number of litters		5				

Figure 3.4 Summary of E9.5 *Smad2* embryos exposed to ATRA. 29% of wild-type and 76% of *Smad2* $^{+/-}$ embryos exhibit abnormalities after ATRA teratogenesis. Analysis was performed by Dr. Tessa Carrel.

Chapter 4

Introduction

The finding that *Tgif* mutations create a susceptibility to ATRA teratogenesis provides indirect evidence that Tgif acts as an inhibitor of RA signaling during embryogenesis. Verifying this possibility requires a method for quantifying levels of retinoic acid signaling in the presence and absence of Tgif. For this objective I employed a *lacZ* reporter gene whose expression is responsive to retinoid signaling, therefore allowing the direct visualization of this signaling. The *lacZ* reporter system is commonly used for these purposes. First, a *β-galactosidase* gene is fused to a promoter of interest. Then, under conditions specific to the promoter, *β-galactosidase* is expressed. Finally the β-galactosidase protein may be stained for, revealing the expression patterning of the promoter.

4.1 Use of a retinoic acid responsive *lacZ* reporter to visualize retinoid signaling in *Tgif* mutants

The *lacZ* strain utilized for this project was obtained from Dr. Anthony LaMantia at the University of North Carolina at Chapel Hill. This strain possesses a randomly inserted *β-galactosidase* gene under the control of an artificial promoter responsive to retinoid signaling. The promoter contains three tandemly fused RAREs taken from the *RARβ-2* gene [35] (Figure 4.1). It has been characterized in both mice and derived cell lines as responsive to ATRA [35]. In mice, embryos exposed to ATRA 14 hours before

staining showed an expanded region of RA signaling in the forebrain and tail at E9.5 and E10.5 [35].

This strain was bred into the *Tgif* mutant background, and embryos were assayed for their RA signaling patterns and levels at E9.5 and E10.5 according to a protocol from Balkan *et al.* [36]. As seen in the characterization by Balkan *et al.*, embryos at this stage produce a pattern of *β-galactosidase* expression in prospective forebrain. This expression is absent along the midline of the prospective forebrain. Extensive expression also occurs along the dorsal midline, extending from the auditory vesicle to the end of the tail [35] (Figure 4.2). This expression pattern is within the origins of the majority of abnormalities seen through ATRA teratogenesis, including HPE, forebrain reductions, and axial defects.

Assuming that *Tgif* functions to inhibit RA signaling during embryogenesis, it is expected that a greater amount of *LacZ* expression will occur in embryos lacking one or two copies of *Tgif*. These expectations were met to a certain extent at both E9.5 and E10.5 stages. However, analysis became confusing when a small portion of *Tgif* ^{wt} embryos showed darker staining than *Tgif* $^{+/-}$ littermates, and likewise with *Tgif* $^{+/-}$ embryos compared to *Tgif* $^{-/-}$ littermates. Upon further examination of the previously mentioned teratogenesis results, it appears that these observations are consistent and may even be expected.

Figure 4.3 is another representation of the teratogenesis results. Each bar represents the portions of normal and abnormal embryos from one of the three genotypes tested. This data shows that 28% of *Tgif* ^{wt} embryos were susceptible to ATRA teratogenesis at the dosage administered. Thus, even without *Tgif* mutations

there is an inherent susceptibility within 28% of wild-type embryos. Furthermore, 48% of *Tgif* $^{+/-}$ embryos showed this susceptibility, where 52% remained normal. As a consequence, it may be assumed that the 28% of wild-type embryos incurring abnormalities possessed a greater inherent susceptibility to ATRA teratogenesis than the 52% of *Tgif* $^{+/-}$ embryos that remained normal. Assuming that greater endogenous levels of RA signaling serve as a readout for teratogenesis susceptibility, it is expected that 15% (28% x 52%) of *Tgif* ^{wt} : *Tgif* $^{+/-}$ comparisons will show greater staining in the wild-type embryo. This assumption also reduces the expected number of *Tgif* ^{wt} : *Tgif* $^{+/-}$ comparisons with greater staining in the *Tgif* $^{+/-}$ embryo from the original 100% down to 35% (48% x 72%). These new expected values leave a large region of gray area because the number of abnormal *Tgif* $^{+/-}$ embryos expected to stain darker than abnormal *Tgif* ^{wt} embryos cannot be determined through the teratogenesis data. This is the same for comparing the normal embryos as well. Therefore, 50% (100% -15% - 35%) of *Tgif* ^{wt} : *Tgif* $^{+/-}$ comparisons cannot be designated as expected greater staining in either embryo.

With new expected values based on teratogenesis data, it is possible to test whether endogenous RA activity levels can predict the predisposition to developing abnormalities through exogenous exposure to ATRA. For validity purposes, a strict system was set up to ascertain results. Because small alterations in staining procedures as well as variances in embryo age result in noticeable differences in staining intensity, embryos were only compared with same-age littermates. In a blind comparison, each embryo was paired with all other littermates and scored as darker or similar staining intensity. Expanded boundaries of staining were also observed, but

always accompanied a darker intensity. Next, genotypes were determined and comparisons were added together by genotype (Table 4.1). Interestingly, pairings of embryos with the same genotype showed a good deal of variability. To be exact, 29% of *Tgif* ^{wt} (n=14), 67% of *Tgif* $^{+/-}$ (n=21) and 50% of *Tgif* $^{-/-}$ (n=6) pairs displayed differing staining intensity. The results for pairs of embryos with different genotypes were analyzed against the expected values obtained from the teratogenesis experiment represented in Chapter 3 in addition to values obtained from the recapitulation of this experiment by Bartholin *et al.* from Dr. David Wotton's laboratory (Table 4.1). The teratogenesis results vary because Bartholin *et al.* used gavage feeding to administer RA instead of intraperitoneal injections. Although the same proportion of RA was given to pregnant mothers, gavage feeding allows for a smaller effective dose exposed to the embryos, resulting in a non-statistically significant increase in susceptibility from *Tgif* $^{+/-}$ to *Tgif* $^{-/-}$. After comparison of observed percentages to minimal expected percentages, only two of six pair groups showed greater *β-galactosidase* expression than the expected minimums from both sets of teratogenesis data. These pair groups were the percentage of *Tgif* $^{+/-}$ embryos with greater expression than *Tgif* ^{wt} embryos ($p<0.01$) and *Tgif* $^{-/-}$ embryos with greater expression than *Tgif* ^{wt} embryos ($p<0.005$). Unfortunately the remaining percentages are too low to carry significance with the small number of parings observed. However, it is clear that even with such a qualitative measure of RA signaling, there is an increase in basal levels of RA signal transduction in mouse embryos possessing one or more null alleles of *Tgif*. These observations support the proposal that Tgif acts as an inhibitor of RA signaling during embryonic development.

4.2 Quantification of *β-galactosidase* expression in *Smad2* mutants

Because *Smad2* mutations parallel *Tgif* mutations in their ability to increase sensitivity to ATRA teratogenesis, Smad2 likely acts as an inhibitor of RA signaling during development as well. In order to investigate this possibility, the RA responsive *lacZ* reporter was bred onto the *Smad2* mutant background. A quantitative analysis of *β-galactosidase* expression was used to compare RA signaling levels between wild-type and *Smad2* $^{+/-}$ embryos at E9.5 and E10.5. As mentioned in Chapter 2, embryos homozygous for a null allele of *Smad2* do not survive to the stage assayed in this analysis. The protocol for quantification of *β-galactosidase* expression in cell extracts was taken from Balkan *et al.* [35]. Once embryos were removed from the mother, the heads were separated from the bodies and assayed. The decapitation was used to avoid the flushing out of subtle differences in the head with the overpowering expression coming from the tail. Subsequently, pair-wise comparisons were made between littermates according to the parameters of the previous experiment. Results show that 72% ($p<0.005$) of pairs showed higher expression in the *Smad2* $^{+/-}$ embryo, and 28% of pairs showed higher expression in the *Smad2* ^{wt} embryo (Figure 4.4). These values were compared to expected values based on the teratogenesis experiments performed on *Smad2* mutant embryos as described in Chapter 3 (Figure 3.4). Results correlate well with the 54% and 7% minimal expected values respectively (Figure 4.4). Furthermore, when litters are examined individually, all but one show an upward trend between the mean *β-galactosidase* expression levels from wild-type to

Smad2 $^{+/-}$ embryos (Figure 4.5). Finally, these results provide evidence for Smad2 as an inhibitor of retinoid signaling during embryogenesis.

4.3 Materials and Methods

4.3.1 Whole mount visualization of *β-galactosidase* expression

After dissection, embryos were fixed in 4% paraformaldehyde with 0.4% glutaraldehyde for 1-2 hours at 4 ^{o}C. Embryos were then washed twice in 1X PBS. Next they were incubated for 45 minutes at room temperature in the absence of light in β-galactosidase staining media (5mM potassium ferricyanide, 5mM potassium ferrocyanide, 1.0mg/ml X-gal, 0.2% NP-40, 2mM $MgCl_2$, diluted in 1X PBS). Finally, embryos were washed twice with 1X PBS and photographed for comparison.

4.3.2 Quantification of *β-galactosidase* expression

After dissection, embryo heads were removed just above the auditory vesicle and placed in 40μl of 1X PROMEGA Reporter Lysis Buffer. After homogenization, 20μl were removed and added to 400μl of Z buffer (60mM $Na_2HPO_4 \bullet 7H_2O$, 40mM $NaH_2PO_4 \bullet H_2O$, 10mM KCl, 1mM $MgSO_4$, 0.27% β –mercaptoethanol, 4.3mM ONPG, pH to 7.0). This solution was incubated at 37 ^{o}C for 6 hours. The reaction was terminated with 200μl of 1M Na_2CO_3, and expression levels were calculated with a spectrophotometer by measuring the absorbancy at λ570. These values were normalized with the protein concentration of each sample, which was measured using the Bio Rad $^{D}_{C}$ Protein Assay.

	Observed	Lasse Expected	Bartholin *et al*. Expected
Total *Tgif* ^{wt} : *Tgif* $^{+/-}$ Pairs	19		
Percent with Higher Expression Level in *Tgif* ^{wt}	5% (1)	15%	12%
Percent with Higher Expression Level in *Tgif* $^{+/-}$	79% (15)	35%	41%
Total *Tgif* ^{wt} : *Tgif* $^{+/-}$ Pairs	32		
Percent with Higher Expression Level in *Tgif* $^{+/-}$	9% (3)	1%	17%
Percent with Higher Expression Level in *Tgif* $^{-/-}$	28% (9)	51%	29%
Total *Tgif* ^{wt} : *Tgif* $^{+/-}$ Pairs	10		
Percent with Higher Expression Level in *Tgif* ^{wt}	0% (0)	1%	9%
Percent with Higher Expression Level in *Tgif* $^{-/-}$	90% (9)	71%	50%

Table 4.1 Comparison of endogenous levels of RA signaling in E9.5 and E10.5 *Tgif* mutant embryos. Embryos possessing a retinoid signaling responsive lacZ reporter allele were stained for B-galactosidase expression at E9.5 and E10.5. Littermates were compared in a blind fashion and scored as showing higher expression levels in either embryo or similar expression levels. Percentages of observed pair differences are represented along with minimum expected percentages extrapolated from teratogenesis data performed by myself and Bartholin *et al*. In parenthesis are the numbers of pairs that correspond to the accompanying percentage values.

Figure 4.1 Retinoic acid responsive *lacZ* reporter allele. The arrows represent RARE sequences taken from the *RARβ-2* promoter and are indicated as positioned forward or backward. These are followed by a TK promoter, a *β-galactosidase* gene, and the construct ends with an SV40 intron plus polyadenylylation site. Taken from [35].

Figure 4.2 Embryos carrying the RA responsive *β-galactosidase* allele after lacZ staining. In this representative example, the *Tgif* $^{+/-}$ embryo on the left displays darker staining than the *Tgif* ^{wt} embryo on the right.

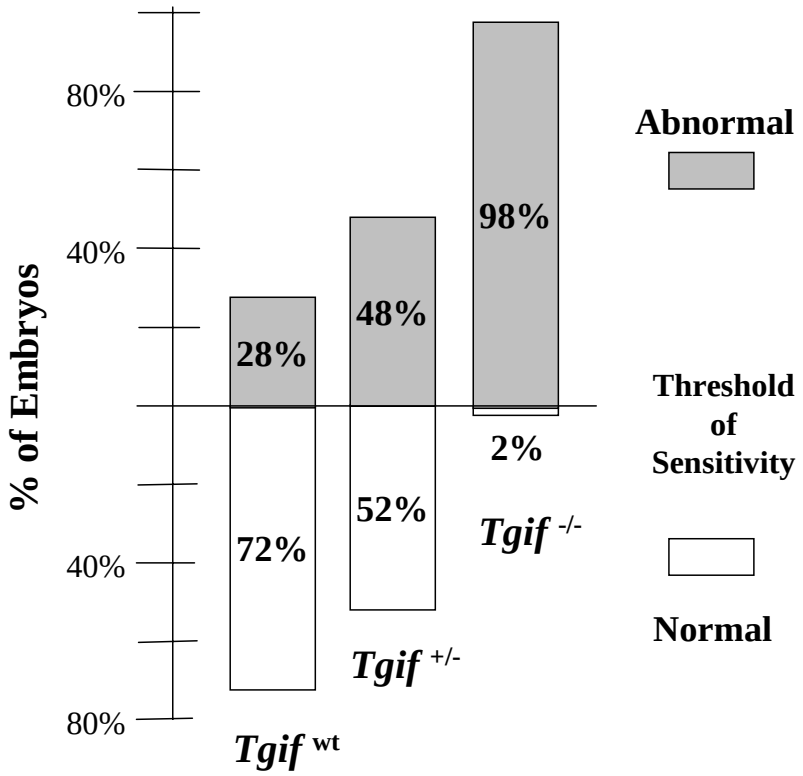

Figure 4.3 Second representation of teratogenesis results.

		Minimum Expected
Total *Smad2* ^{wt} vs. *Smad2* $^{+/-}$ Pairs	36	
Percent With Higher Expression Level in *Smad2* ^{wt}	28% (10)	7%
Percent With Higher Expression Level in *Smad2*$^{+/-}$	72% (26)	54%

Figure 4.4 Comparison of endogenous levels of RA signaling in E9.5 and E10.5 *Smad2* mutant embryos. Cranial tissue of embryos possessing a retinoid signaling responsive *lacZ* reporter allele was quantified for *β-galactosidase* expression at E9.5 and E10.5. Percentages of observed pair differences are represented along with minimum expected percentages taken from teratogenesis data performed by Dr. Tessa Carrel. In parenthesis are the numbers of pairs that correspond to the accompanying percentage values.

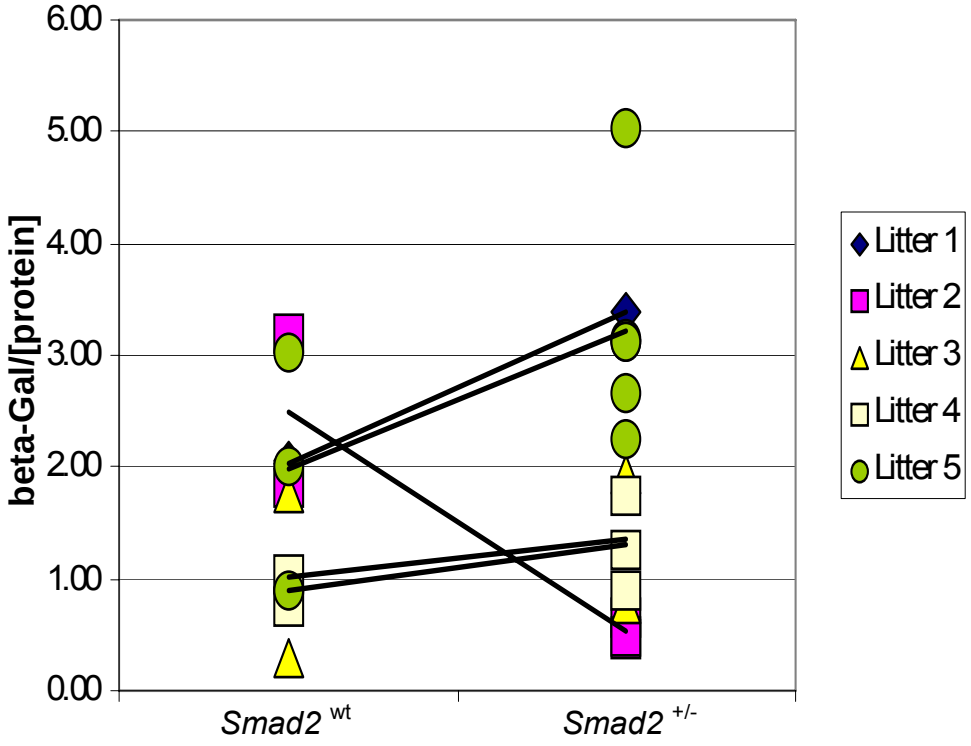

Figure 4.5 Litterwise comparison of *β-galactosidase* expression in wild-type and *Smad2* mutant embryos. Quantified β-galactosidase levels were normalized using the protein concentration of each sample, which correspond to the values on the Y-axis. Embryos are separated by genotype. Each embryo is represented by a symbol corresponding to the litter number, and black trend lines connect mean expression values of wild-type and *Smad2* $^{+/-}$ embryos of each litter. Four of five litters show higher mean expression in *Smad2* heterozygous over wild-type embryos.

Chapter 5

Introduction

After demonstrating that haploinsufficiency of *Smad2* increases susceptibility to ATRA teratogenesis, I proceeded to investigate a potentially novel interaction between TGF-β and retinoid signaling pathways. If, as predicted from these observations, TGF-β signals are able to inhibit retinoid signaling through the TGF-β signal transducer Smad2, then there are a number of stages throughout the process of retinoid signaling that Smad2 may produce its affects. The most likely of these stages is at the level of the retinoid receptors. As mentioned in Chapter 1, the RAR and RXR families of proteins each contain three isoforms (α,β,γ) with a number of splicing variants (reviewed in [15]). The large number of possible heterodimers and homodimers provide a great deal of complexity, requiring an equivalent amount of regulation to carry out the variety of functions performed by RA signaling during development. A 2003 publication by a group in Paris, France, showed that Smad3, highly homologous to Smad2, is able to bind RAR-γ *in vitro* [37]. This interaction was also shown to facilitate an enhancement of Smad3 dependent transcription [37]. Fortunately I was given the opportunity to travel to Paris and investigate the binding of Smad2 to RAR-γ in addition to the effect of Smad2 on retinoid dependent transcription.

5.1 Use of immunoprecipitation to assess physical interactions between Smad2 and RAR-γ proteins

For the elucidation of any physical interaction between Smad2 and RAR-γ, both a Myc-tagged Smad2 and Gal4-tagged RAR-γ were overexpressed in 293T cells. An immunoprecipitation assay was then performed, pulling down Gal4-RAR-γ and blotting for Myc-Smad2 with anti-Gal4 and anti-Myc antibodies respectively. Unlike Smad3, however, no evidence was found for the interaction between Smad2 and RAR-γ (data not shown). Dr. David Wotton's group later repeated these results.

As a direct result of my teratogenesis findings the Wotton group also tested interactions between Tgif and RAR or RXR proteins. Not surprisingly, they showed a strong interaction between Tgif and RXR-α (Bartholin *et al.* unpublished data). This interaction was found under conditions of overexpression and at endogenous levels.

5.2 Use of semi-quantitative RT-PCR to measure Smad2 regulation of *RAR* and *RXR* transcription

Despite ruling out a physical interaction between Smad2 and one of three retinoic acid receptors, many other possible methods remain for Smad2 to deliver its effects on retinoid signaling. These effects may occur at the transcriptional, translational, or functional stages of retinoid receptor activity. To this end, I decided to first investigate the ability of Smad2 to influence the transcription of the three RAR isoforms and three RXR isoforms. Semi-quantitative RT-PCR techniques were utilized for this purpose. HepG2 cells were transiently transfected with Smad2 or an empty vector as a control,

and endogenous transcription levels of each of the RARs and RXRs were measured. Upregulation of *Smad2* was verified through RT-PCR analysis, and primers for GAPDH were used to ensure even sample loading. This assay also acts as a read-out for Smad2's regulation of RA signaling, as many of the RAR's and RXR's contain retinoid responsive elements in their promoters [38]. After repeated attempts, it was determined that the levels of RAR and RXR transcript were unaltered by the presence of exogenous Smad2 (data not shown).

5.3 Use of a retinoic acid responsive luciferase reporter to measure the affect of Smad2 on retinoid regulated transcription

Finally, I decided to test the functional stage of RAR and RXR activity. By observing the last step of retinoid receptor function, I should be able to elucidate whether Smad2 is able to influence RA signaling at any point upstream in the pathway. For this purpose, HepG2 and 293T cells were transiently transfected with an RA responsive luciferase reporter. This reporter contains three tandemly repeated RAREs in its promoter, similar to the previously described RA responsive *lacZ* reporter and is likewise responsive to treatment with ATRA. Luciferase activity was measured in the presence or absence of Smad2, Smad4, ATRA, and TGF-β ligand. Expression of *Smad2* and *Smad4* were verified through western blotting (data not shown). Despite apparent changes in luciferase activity in single experiments, such alterations were not consistently repeatable. Thus it seems that Smad2 is unable to affect retinoid signaling *in vitro*. These negative findings may be a context dependent result due to the cell types used or specific to the promoter chosen for the experiment.

5.4 Materials and Methods

5.4.1 Cell Culture

HepG2 and 293T cells were grown in Dulbecco's modified Eagle's medium (DMEM) supplemented with 10% heat-inactivated fetal calf serum (FCS), 2mM glutamine and antibiotics (100 U/ml penicillin, 50 mg/ml streptomycin G, and 0.25 mg/ml Fungizone^{TM}). Cells were maintained at 37 ^{o}C in a 5% CO_2 – 95% air atmosphere.

5.4.2 Transient cell transfections

Transient cell transfections were performed using a jetPEI kit from QBIOGENE. In experiments requiring the addition of ATRA or TGF-β ligand, cultures were placed in DMEM containing 1% FCS before treatment. Human recombinant TGF-β ligand was purchased from R&D Systems Inc. All-trans retinoic acid (ATRA) was purchased from Sigma. In every experiment an eGFP vector was cotransfected to monitor transfection efficiencies.

5.4.3 Immunoprecipitation and western blotting

Myc-tagged Smad2 and Gal4-tagged RAR-γ expression vectors were transfected into 293T cells. After 48 hours, cells were washed twice with cold 1X PBS, scraped, and dissolved in Buffer N (50mM Tris-HCl, pH 7.5, 150mM NaCl, 2mM EDTA, 1% NP-40). Lysates were then cleared of debris by centrifugation, and incubated with protein G-sepharose beads at 4 ^{o}C for 1 hour to remove non-specific binding proteins

(Amersham Biosciences). Next they were incubated with an anti-Gal4 antibody (Santa-Cruz Biotech) overnight at 4 ^{o}C, followed by another incubation with protein G–sepharose beads at 4 ^{o}C for 1 hour. After washing the pellet twice with buffer N and twice with PBS, immunoprecipitates were eluted by boiling for 3 minutes and subjected to SDS–polyacrylamide gel electrophoresis. Proteins were then transferred to a nitrocellulose membrane and immunoblotted with an anti-Myc (Roche) antibody. Protein bands were visualized using the ECLplus Western Blotting Detction System® from Amersham Biosciences.

5.4.4 Semi-quantitative RT-PCR

RNA extraction was performed using to the RNeasy® Mini Kit from QIAGEN. cDNA libraries were then prepared. Semi-quantitative PCR was performed on the cDNAs to measure levels of RAR-α,β,γ and RXR-α,β,γ transcription. Human gene sequences were obtained from www.ensembl.org. RAR-α was amplified using published primers [39]. The remaining gene specific primers were designed using Primer Premier software from Biosoft International. All primers were made to cross intron/exon boundaries. The primer sequences and product lengths are indicated in Table 5.1. Multiplex PCR was performed using the Multipex PCR Kit from QIAGEN. Products were separated by gel electrophoresis and visualized with ethidium bromide staining.

5.4.5 Luciferase assays

A synthetic retinoid responsive promoter tagged to a luciferase reporter gene was transfected into HepG2 and 293T cells along with vectors containing components of TGF-β signaling. As an internal expression control, a vector containing the renilla reporter gene under the control of a TK-promoter was cotransfected in every experiment. After 6 hours of incubation at 37 ^{o}C, cultures were placed in DMEM containing 1% FCS, at which time ATRA was added to designated cultures at a concentration of 1μM. After 16 more hours of incubation, TGF-β ligand was added to designated cultures at a concentration of 5ng/ml. After a final 2-hour incubation, cells were washed twice with 1X PBS and assayed for luciferase and renilla expression using the Luclite® and Renlite® Reporter Gene Assay Systems from PerkinElmer. *Smad2* and *Smad4* vectors were tagged with a Flag epitope tag and expression was verified through western blotting as described above, using anti-Flag antibodies from Sigma.

Gene Name	Forward Primer	Reverse Primer	Product Length
RXR-α	5'-ATACGTGGAGGCAAACATGG-3'	5'-TAGCACCCTGTCAAAGATGG-3'	307bp
RXR-β	5'-GCAAGCACTATGGGGTTTAC-3'	5'-TAGTCACTGGGTCATTTGGG-3'	372bp
RAR-α	5'-ATCGAGACCCAGAGCAGCAG-3'	5'-CCTGGTGCGCTTTGCGAACC-3'	420bp
RAR-β	5'-CAGAAGTGCTTTGAAGTGGG -3'	5'-AACACAAGGTCAGTCAGAGG-3'	494bp
RXR-γ	5'-AGACAGAATCCTACGGTGAC-3'	5'-GTGTTCCAGGCATTTCAAGC-3'	563bp
RAR-γ	5'-AACTCATCACCAAGGTCAGC-3'	5'-TTCTGCTCCCTTAGTGCTGA-3'	623bp

Table 5.1 List of primers used for semi-quantitative RT-PCR.

Chapter 6

Discussion

Many human birth defects have been studied through the use of mouse models. Holoprosencephaly (HPE), a range of forebrain and craniofacial abnormalities resulting in a high incidence of lethality, has been no exception. Many teratogens and genetic mutations have been shown to cause HPE; one such teratogen is retinoic acid (RA). Exposure of pregnant females to exogenous RA has been observed to cause HPE in both humans and mice [32, 33].

One gene that has been found mutated in a number of human cases of HPE is *TGIF* (TG interacting factor) (reviewed in [6]). This gene encodes a homeobox domain protein, identified through its ability to repress RA signaling through binding of the retinoid X receptor response element [11]. Tgif also functions in TGF-β signaling [19]. Interestingly, mice homozygous for null mutations in *Tgif* do not exhibit HPE. However, teratogenesis experiments reveal that mutations in *Tgif* render mice more susceptible to ATRA teratogenesis. This increased susceptibility relates to the total range of abnormalities caused by exogenous ATRA as well as the incidence of HPE specifically. These findings represent a novel cooperation between genetic and environmental factors in the development of HPE.

Using a *lacZ* reporter allele under the influence of a RA responsive promoter, I investigated whether the loss of *Tgif* or *Smad2* is able to raise endogenous levels of retinoic acid signaling. I found through visual analysis of *β-galactosidase* expression that a significant percentage of *Tgif* $^{+/-}$ and *Tgif* $^{-/-}$ embryos show greater RA signaling levels than wild-type littermates. Using a *β-galactosidase* quantification assay, cranial RA signaling was measured in *Smad2* embryos. Again, a significant increase in signaling was found in *Smad2* $^{+/-}$ compared to wild-type littermates. These results support the *in vitro* evidence that Tgif acts as a repressor of RA signal transduction [11] and suggest a novel interaction between *Smad2* and RA signaling. Furthermore, greater levels of endogenous retinoid signaling may foreshadow increased susceptibility to ATRA teratogenesis, as suggested through the correlation of *β-galactosidase* expression comparisons with ATRA teratogenesis data. However, greater numbers of pairs need to be observed to provide statistically significant evidence for this conclusion.

Although a mechanism has already been proposed for the ability of Tgif to repress retinoid signaling ([11], Bartholin *et al*. unpublished data), Smad2 has not previously been characterized as having such activity. Because the most likely point of retinoid signaling repression lies with the activity of the retinoid receptors, *in vitro* assays were designed to test this hypothesis. Unfortunately, any mechanisms by which Smad2 represses retinoid signaling remain elusive, as immunoprecipitations failed to demonstrate binding between Smad2 and RAR-γ, RAR and RXR transcription is not altered by the presence of Smad2, and Smad2 was unable to regulate the function of RARs and RXRs in the promotion of retinoid dependent transcription.

Works Cited

1. Volpe, J.J., *Overview: normal and abnormal human brain development.* Ment Retard Dev Disabil Res Rev, 2000. **6**(1): p. 1-5.

2. Matsunaga, E. and K. Shiota, *Holoprosencephaly in human embryos: epidemiologic studies of 150 cases.* Teratology, 1977. **16**(3): p. 261-72.

3. Roach, E., et al., *Holoprosencephaly: birth data, benetic and demographic analyses of 30 families.* Birth Defects Orig Artic Ser, 1975. **11**(2): p. 294-313.

4. Demyer, W., W. Zeman, and C.G. Palmer, *The Face Predicts the Brain: Diagnostic Significance of Median Facial Anomalies for Holoprosencephaly (Arhinencephaly).* Pediatrics, 1964. **34**: p. 256-63.

5. Muenke, M., *Holoprosencephaly as a model for normal craniofacial development.* seminars in Developmental Biology, 1994. **5**: p. 293-301.

6. Wallis, D.E. and M. Muenke, *Molecular mechanisms of holoprosencephaly.* Mol Genet Metab, 1999. **68**(2): p. 126-38.

7. Roelink, H., et al., *Floor plate and motor neuron induction by different concentrations of the amino-terminal cleavage product of sonic hedgehog autoproteolysis.* Cell, 1995. **81**(3): p. 445-55.

8. Ming, J.E. and M. Muenke, *Holoprosencephaly: from Homer to Hedgehog.* Clin Genet, 1998. **53**(3): p. 155-63.

9. Belloni, E., et al., *Identification of Sonic hedgehog as a candidate gene responsible for holoprosencephaly.* Nat Genet, 1996. **14**(3): p. 353-6.

10. Chiang, C., et al., *Cyclopia and defective axial patterning in mice lacking Sonic hedgehog gene function.* Nature, 1996. **383**(6599): p. 407-13.

11. Bertolino, E., et al., *A novel homeobox protein which recognizes a TGT core and functionally interferes with a retinoid-responsive motif.* J Biol Chem, 1995. **270**(52): p. 31178-88.

12. Gripp KW, E.M., Mowat D, Meinecke P, Richieri-Costa A, Zackai EH, Elledge S, Muenke M., *Mutations in the transcription factor TGIF in holoprosencephaly.* American Journal of Human Genetics, 1998. **63**(A32).

13. Cohen, M.M., Jr. and K. Shiota, *Teratogenesis of holoprosencephaly.* Am J Med Genet, 2002. **109**(1): p. 1-15.

14. Gilbert, S.F., *Developmetnal Biology*. 6th ed. 2000, Sunderland: Sinauer Associates, Inc.

15. Chambon, P., *A decade of molecular biology of retinoic acid receptors.* Faseb J, 1996. **10**(9): p. 940-54.

16. Wolf, G., *The regulation of retinoic acid formation.* Nutr Rev, 1996. **54**(6): p. 182-4.

17. Alberts, B.J., Alexander; Lewis, Julian; Raff, Martin; Roberts, Keith; Walter, Peter, *Molecular Bioloby of the Cell*. 4th ed. 2002, New York: Garland Publishing.

18. Abe, Y., T. Minegishi, and P.C. Leung, *Activin receptor signaling.* Growth Factors, 2004. **22**(2): p. 105-10.

19. Wotton, D., et al., *A Smad transcriptional corepressor.* Cell, 1999. **97**(1): p. 29-39.

20. Luo, K., et al., *The Ski oncoprotein interacts with the Smad proteins to repress TGFbeta signaling.* Genes Dev, 1999. **13**(17): p. 2196-206.

21. Pessah, M., et al., *c-Jun associates with the oncoprotein Ski and suppresses Smad2 transcriptional activity.* J Biol Chem, 2002. **277**(32): p. 29094-100.

22. Gehring, W.J., M. Affolter, and T. Burglin, *Homeodomain proteins.* Annu Rev Biochem, 1994. **63**: p. 487-526.

23. Purves, D.A., George.J.; Fitzpatrick, David; Katz, Lawrence.C.; LaMantia, Anthony-Samuel.; McNamara, James.O.; Williams, S. Mark, *Neuroscience*. 2nd ed. 2001, Sunderland: Sinauer Associates, Inc.

24. Nambu, P.A. and J.R. Nambu, *The Drosophila fish-hook gene encodes a HMG domain protein essential for segmentation and CNS development.* Development, 1996. **122**(11): p. 3467-75.

25. Sanchez-Soriano, N. and S. Russell, *Regulatory mutations of the Drosophila Sox gene Dichaete reveal new functions in embryonic brain and hindgut development.* Dev Biol, 2000. **220**(2): p. 307-21.

26. Mukherjee, A., et al., *The Drosophila sox gene, fish-hook, is required for postembryonic development.* Dev Biol, 2000. **217**(1): p. 91-106.

27. Weinstein, M., et al., *Failure of egg cylinder elongation and mesoderm induction in mouse embryos lacking the tumor suppressor smad2.* Proc Natl Acad Sci U S A, 1998. **95**(16): p. 9378-83.

28. Liu, Y., et al., *Smad2 and Smad3 coordinately regulate craniofacial and endodermal development.* Dev Biol, 2004. **270**(2): p. 411-26.

29. Gripp, K.W., et al., *Mutations in TGIF cause holoprosencephaly and link NODAL signalling to human neural axis determination.* Nat Genet, 2000. **25**(2): p. 205-8.

30. Yang, X., et al., *Targeted disruption of SMAD3 results in impaired mucosal immunity and diminished T cell responsiveness to TGF-beta.* Embo J, 1999. **18**(5): p. 1280-91.

31. Nau, H., *Embryotoxicity and teratogenicity of topical retinoic acid.* Skin Pharmacol, 1993. **6 Suppl 1**: p. 35-44.

32. Lammer, E.J., et al., *Retinoic acid embryopathy.* N Engl J Med, 1985. **313**(14): p. 837-41.

33. Sulik, K.K., et al., *Teratogenicity of low doses of all-trans retinoic acid in presomite mouse embryos.* Teratology, 1995. **51**(6): p. 398-403.

34. Sucov, H.M., et al., *Mouse embryos lacking RXR alpha are resistant to retinoic-acid-induced limb defects.* Development, 1995. **121**(12): p. 3997-4003.

35. Balkan, W., et al., *Transgenic indicator mice for studying activated retinoic acid receptors during development.* Proc Natl Acad Sci U S A, 1992. **89**(8): p. 3347-51.

36. Balkan, W., et al., *Transgenic mice expressing a constitutively active retinoic acid receptor in the lens exhibit ocular defects.* Dev Biol, 1992. **151**(2): p. 622-5.

37. Pendaries, V., et al., *Retinoic acid receptors interfere with the TGF-beta/Smad signaling pathway in a ligand-specific manner.* Oncogene, 2003. **22**(50): p. 8212-20.

38. De Luca, L.M., *Retinoids and their receptors in differentiation, embryogenesis, and neoplasia.* Faseb J, 1991. **5**(14): p. 2924-33.

39. Boylan, J.F., et al., *Targeted disruption of retinoic acid receptor alpha (RAR alpha) and RAR gamma results in receptor-specific alterations in retinoic acid-mediated differentiation and retinoic acid metabolism.* Mol Cell Biol, 1995. **15**(2): p. 843-51.